Journal of Medicinal Chemistry

Article

pubs.acs.org/jmc

Design of Specific Serine Protease Inhibitors Based on a Versatile Peptide Scaffold: Conversion of a Urokinase Inhibitor to a Plasma Kallikrein Inhibitor

Peng Xu,[†] Mingming Xu,[‡] Longguang Jiang,[‡] Qinglan Yang,[†] Zhipu Luo,[§] Zbigniew Dauter,[§] Mingdong Huang,[‡] and Peter A. Andreasen*[,†]

[†]Danish-Chinese Centre for Proteases and Cancer, Department of Molecular Biology and Genetics, Aarhus University, Aarhus, 8000, Denmark

[‡]Danish-Chinese Centre for Proteases and Cancer, Fujian Institute of Research on the Structure of Matter, Chinese Academy of Sciences, Fuzhou, 350002, China

[§]Synchrotron Radiation Research Section, Macromolecular Crystallography Laboratory, National Cancer Institute, Argonne National Laboratory, Argonne, Illinois 60439, United States

Supporting Information

ABSTRACT: All serine proteases hydrolyze peptide bonds by the same basic mechanism and have very similar active sites, in spite of the fact that individual proteases have different physiological functions. We here report a strategy for designing high-affinity and high-specificity serine protease inhibitors using a versatile peptide scaffold, a 10-mer peptide, mupain-1 (CPAYSRYLDC). Mupain-1 was previously reported as a specific inhibitor of murine urokinase-type plasminogen activator (K_i = 0.55 μM) without measurable affinity to plasma kallikrein (K_i > 1000 μM). On the basis of a structure-based rational design, we substituted five residues of mupain-1 and converted it to a potent plasma kallikrein inhibitor (K_i = 0.014 μM). X-ray crystal structure analysis showed that the new peptide was able to adapt a new set of enzyme surface interactions by a slightly changed backbone conformation. Thus, with an appropriate re-engineering, mupain-1 can be redesigned to specific inhibitors of other serine proteases.

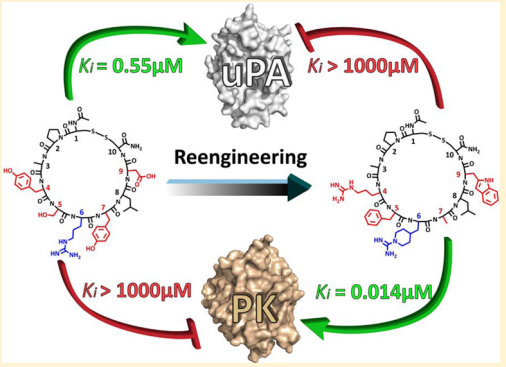

INTRODUCTION

Trypsin-like serine proteases catalyze the hydrolysis of peptide bonds and are involved in numerous physiological pathways, including digestion, blood clotting, fibrinolysis, complement activation, and turnover of extracellular matrix.[1] All serine proteases of the trypsin clan catalyze the same type of hydrolytic reaction by the same biochemical mechanism and have similar active sites. Nevertheless, these serine proteases have highly variable and sometimes opposite physiological functions, like the complementary functions of thrombin and plasmin. Serine proteases have been shown to be successful therapeutic targets for a number of pathological conditions.[2,3] Serine protease inhibitors are clinically used for therapy of several maladies, including thrombosis and unregulated bleeding.[4] A high specificity of protease inhibitors is crucial, as off-target effects can give rise to severe systemic disorders. One example illustrating the importance of inhibitor specificity is the failure of clinical trials of nonspecific matrix metalloprotease inhibitors as anticancer drugs.[5] In spite of strong structural similarity of their active sites, different matrix metalloproteases are now known to have very different physiological and pathophysiological functions.[6] Nonspecific inhibitors targeting all about 25 different matrix metalloproteases could thus have both anticancer and procancer effects.

All serine proteases of the trypsin family have a catalytic triad (His57, Asp102, and Ser195, chymotrypsinogen numbering) in the center of the active site. Besides, the active site also consists of the S1 specificity pocket which accommodates the side chain of the P1 residue, and the oxyanion hole composed of the amido groups of Ser195 and Gly193. The binding of the P1 residue into the S1 pocket and its carbonyl oxygen atom into the oxyanion hole ensures the stabilization of the tetrahedral intermediate formed following a nucleophilic attack by the oxygen atom of the hydroxyl group of Ser195 and its stabilization into an acyl enzyme intermediate. Following the release of the P1′ residue, a water molecule performs a second nucleophilic attack, thereby completing the catalytic cycle. However, although serine proteases have high similarity in the active sites, most serine proteases are specific for particular physiological substrates. So the exosites of serine proteases are decisive for the enzyme−substrate recognition and recognition by the enzymes of their physiological serpin and standard

Received: June 26, 2015

ACS Publications © XXXX American Chemical Society

DOI: 10.1021/acs.jmedchem.5b01128
J. Med. Chem. XXXX, XXX, XXX−XXX

mechanism inhibitors.[7,8] It follows that it is easier to achieve specificity with artificial inhibitors binding not only to the active site but also to exosites, i.e., sites outside the S1 pocket and the catalytic triad and the oxyanion hole.[9,10] Small molecule inhibitors targeting only the active sites of enzymes in particular pose specificity problems, but peptides, of a size of about 10−20 amino acids, are more likely to be able to bind to exosites as well as to the active sites and thus be more specific.[11] Peptides are attracting increasing interest as drug candidates for combining the advantages of small molecules (cost, conformational restriction, metabolic stability) with those of proteins (specificity, high potency).[11] Also in the case of serine proteases, peptides are of considerable interest as inhibitors[12−15] and can, in fact, also be used to stimulate the activity of proteases.[16−18]

In our previous work, a 10-mer monocyclic, disulfide bond-constrained peptide, mupain-1 (CPAYSRYLDC), was isolated from a phage-displayed peptide library.[19] Mupain-1 competitively inhibits the activity of urokinase-type plasminogen activator (uPA) from mouse (muPA) with a K_i value of 0.55 μM and shows no measurable or negligible inhibition of other serine proteases tested. Besides blocking the active site, mupain-1 forms a large area of interactions with exosite residues of a muPA.[20] Therefore, we considered if we could retarget mupain-1 to other serine proteases by modulating the peptide−protease interactions. As an example, by rationally changing the residues interacting with the exosites of muPA, we now successfully re-engineered mupain-1 to a specific inhibitor of another trypsin-like serine protease, plasma kallikrein (PK), which is a clinical target of hereditary angioedema.[21] The engineered peptide has completely lost the inhibitory capability to human uPA (huPA) and muPA while having high affinity to human PK (hPK) and murine PK (mPK). X-ray crystal structures and site-directed mutagenesis analysis verified our designing procedure. Together with the enzymological results and surface plasmon resonance (SPR) analysis, we elucidated the binding and inhibitory mechanism of the engineered PK inhibitor. On the basis of our previous and current work, we suggest a principle for designing high-affinity and high-specificity inhibitors of trypsin-like serine proteases by using mupain-1 as a scaffold.

RESULTS AND DISCUSSION

Retargeting Mupain-1 from a muPA Inhibitor to a PK Inhibitor. The P1 residue is a critical residue for peptidic protease inhibitors, since it directly blocks the active site and thus prevents the docking of substrates. We previously synthesized a non-natural arginine analogue, L-3-(*N*-amidino-4-piperidyl)alanine as an improved P1 residue (Figure 1). Substituting the P1 residue (Arg6) of mupain-1 with L-3-(*N*-amidino-4-piperidyl)alanine resulted in peptide mupain-1-16 (CPAYS[L-3-(*N*-amidino-4-piperidyl)alanine]YLDC), which showed a 10-fold lower K_i for inhibition of muPA (Figure 2).[22] In this work, we found L-3-(*N*-amidino-4-piperidyl)alanine significantly improved the inhibitory capability of mupain-1 to hPK and mPK, resulting in K_i values of 1.58 and 4.61 μM, respectively (Figure 1, Table 1). Accordingly, mupain-1-16 was used as a template for the following re-engineering of exosite interactions.

In previous studies, we crystallized mupain-1-16 in complex with a muPA-like, human uPA mutant, huPA-H99Y (PDB code 4X1N). From the crystal structure, we identified the residues of huPA-H99Y that interact with mupain-1-16. By comparing

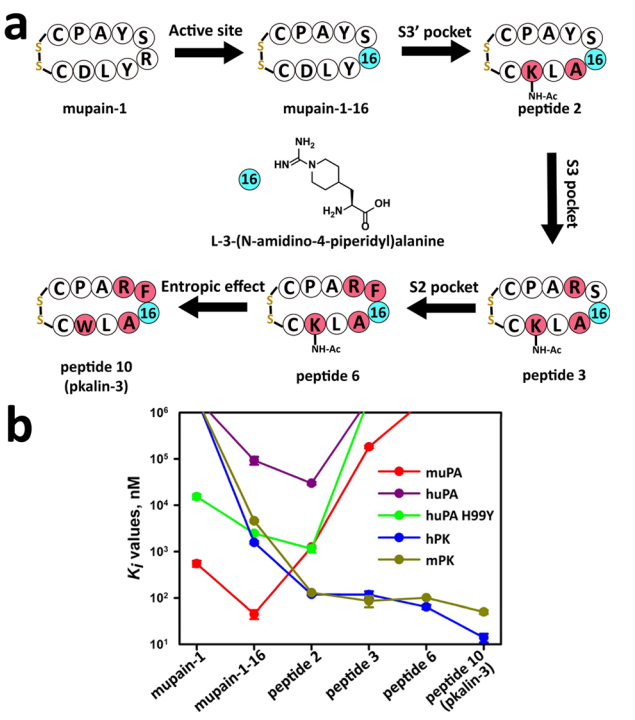

Figure 1. (a) A five-step re-engineering converts the specificity of peptides from muPA to hPK. The structure of the non-natural arginine analog, L-3-(*N*-amidino-4-piperidyl)alanine, is shown in the middle. (b) K_i values of each of the peptides for inhibition of muPA (red), huPA (violet), huPA-H99Y (green), hPK (blue), and mPK (dark yellow) are plotted against the peptide names. Values are represented as the mean ± SD. For clarity, peptides 1, 4, 5, and 7 have been omitted from the figure.

these residues to the corresponding residues in hPK, we found three critical differences in the peptide binding regions: the S3′ pocket, the S3 pocket, and the S2 pocket (Figure 2). We hypothesized that mupain-1-16 bound to hPK and huPA-H99Y in a similar conformation. So the specific residues of mupain-1-16 would interact with the same regions of hPK and of huPA-H99Y. Therefore, according to these differences, we performed a stepwise substitution of mupain-1-16 residues that interact with the exosites of huPA-H99Y. The purpose of each step was to optimize the binding of the peptide to hPK and decrease the peptides' affinity to muPA (Figure 1).

The S3′ Pocket. The crystal structure of mupain-1-16:huPA H99Y complex shows that the P1′ residue (Tyr7) of mupain-1-16 forms a hydrogen bond with Arg35 in the S3′ pocket of huPA-H99Y (Figure 2b). But hPK has a nonpolar Val in position 35 (Figure 2b and Figure 2e). We therefore assumed that the bulky Tyr could bring about steric hindrance when binding to hPK and therefore mutated Tyr7 to Ala, resulting in peptide **1** (CPAYS[L-3-(*N*-amidino-4-piperidyl)alanine]-ALDC), which has a 10-fold lower K_i for inhibition of hPK and a slightly higher K_i for inhibition of muPA (Table S2). Another important difference of huPA-H99Y and hPK is that the S3′ pocket of huPA is polar, while the S3′ pocket of hPK is more hydrophobic (Figure 2e). The four tandem positive residues (RRHR) in huPA are compatible with the binding of the negatively charged Asp9 of mupain-1-16. We therefore replaced Asp9 by the nonpolar residue acetyl lysine (KAc) to break the salt bridge and increase the hydrophobicity. The substitution of Asp9 of peptide **1** with acetyl Lys led to peptide **2** (CPAYS[L-3-(*N*-amidino-4-piperidyl)alanine]AL[KAc]C),

DOI: 10.1021/acs.jmedchem.5b01128
J. Med. Chem. XXXX, XXX, XXX−XXX

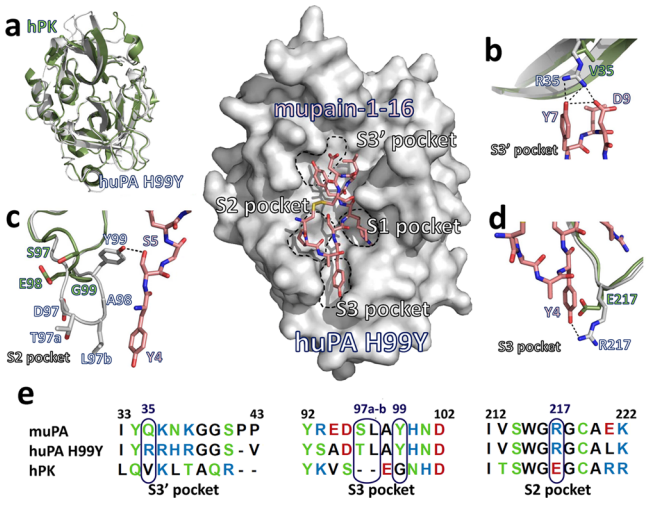

Figure 2. Engineering the exosite interactions in order to retarget mupain-1-16's specificity from uPA to plasma kallikrein. Center: An overview of the crystal structure of mupain-1-16 (salmon sticks) in complex with the catalytic domain of huPA-H99Y (white surface). (a) The backbone conformations of the catalytic domains of huPA-H99Y (white cartoon) and hPK (smudge cartoon) are highly similar. (b–d) Three critical regions of the huPA-H99Y (white cartoon) in complex with mupain-1-16 (salmon sticks): S3′ pocket (b), S3 pocket (c), and S2 pocket (d). The corresponding regions of hPK (smudge cartoon, PDB code 2AYN) are overlaid with huPA-H99Y for comparison. The residues of the two proteases that are critical for binding of mupain-1-16 are shown as sticks. Hydrogen bonds are shown as black dash lines. (e) Alignment of sequences of the S3′ pocket, the S3 pocket, and the S2 pocket of muPA, huPA-H99Y, and hPK; residues are colored according to the properties (black, hydrophobic; green, neutrally polar; blue, positively charged; red, negatively charged).

which has a slightly improved affinity to hPK but an about 10-fold weakened affinity to muPA, with a K_i value up in the μM range (Figure 1 and Table S2).

The S3 Pocket. In the crystal structure, the P3 residue (Tyr4) of mupain-1-16 docks into the S3 pocket and forms a hydrogen bond with Arg217 (Figure 2d). In contrast to the positively charged Arg217 in both human and murine uPA, a negative Glu is present at position 217 of hPK (Figure 2e). Therefore, substituting Tyr4 of peptide **2** with a positive Arg (peptide **3**, CPARS[L-3-(*N*-amidino-4-piperidyl)alanine]AL-[KAc]C) or Lys (peptide **4**, CPAKS[L-3-(*N*-amidino-4-piperidyl)alanine]AL[KAc]C) (Table S2) would be expected to establish an electrostatic attraction with Glu217 of hPK but lead to an electrostatic repulsion from Arg217 in uPAs. Going from peptide **2** to peptide **3** or peptide **4**, a 100-fold increase in K_i for muPA and huPA-H99Y was achieved, but there was no improvement of the affinity to PK. Hereby, Arg was preferred as the P3 residue because of the slightly higher affinity to PK of the Arg-containing peptide **3** than of the Lys-containing peptide **4** (Figure 1 and Table S2).

The S2 Pocket. The crystal structure also shows that the P2 residue of mupain-1-16, Ser5, forms a hydrogen bond with Tyr99 in the 97-loop in the S2 pocket of huPA-H99Y (Figure 2c). Compared to hPK, the human uPA and murine uPA have a sterically narrower S2 pocket because the 97-loops of the uPAs are two residues longer (Thr97a and Leu97b) than the 97-loop of the hPK. Furthermore, the uPAs have bulky residues at position 99 (Tyr99 in muPA and His99 in huPA), while the hPK has only a small Gly99 in the same position (Figure 2c and Figure 2e). The small and hydroxyl-containing Ser5 of mupain-1-16 can easily insert into the narrow S2 pocket of muPA and form a hydrogen bond with Tyr99. To remove this interaction, we tried to substitute Ser5 with either of several nonpolar amino acids, Ala (peptide **5**), Phe (peptide **6**), or Leu (peptide **7**) (Table S2). Among these, the peptide with the highest affinity was the Phe-containing peptide **6** (CPARF[L-3-(*N*-amidino-4-piperidyl)alanine]AL[KAc]C). Peptide **6** has a K_i value for inhibition of hPK of 0.064 μM and has lost any measurable inhibition of uPAs (K_i > 1000 μM). Thus, Phe was chosen as the P2 residue for inhibitors of the hPK, and peptide **6** was used as a scaffold for further modification (Figure 1 and Table S2).

After the three-step structure-based engineering of the exosite interactions, we had completely switched mupain-1-16 to an hPK inhibitor. We further improved the affinity to hPK and mPK by replacing the acetylated Lys in position 9 of the peptide with aromatic residues (Phe and Trp), since the high rigidity of aromatic residues would be expected to result in a more favorable binding entropy.[23] Indeed, peptides **8** (CPARF-[L-3-(*N*-amidino-4-piperidyl)alanine]ALFC) and **10** (CPARF-[L-3-(*N*-amidino-4-piperidyl)alanine]ALWC) showed very high affinities to hPK, with K_i values of 0.008 and 0.014 μM, respectively (Figure 1 and Table S2). Peptide **9** (CPKRS[L-3-(*N*-amidino-4-piperidyl)alanine]ALFC), which has a Lys at position 3, was selected as another promising PK inhibitor with a K_i of 0.022 μM.

Table 1. Specificity of Peptides toward Various Serine Proteases

	K_i (μM)				
protease[a]	mupain-1	mupain-1-16	peptide **8**	peptide **9**	peptide **10**
human PK	>1000	1.58 ± 0.11 (3)	0.008 ± 0.001 (3)	0.022 ± 0.006 (3)	0.014 ± 0.001 (3)
murine PK	>1000	4.61 ± 0.16 (3)	0.027 ± 0.002 (3)	0.043 ± 0.002 (3)	0.050 ± 0.005 (3)
human uPA	>1000[b]	93 ± 18 (3)[b]	>1000	>1000	>1000
murine uPA	0.55 ± 0.08 (3)[b]	0.045 ± 0.01 (4)[b]	>1000	>1000	>1000
bovine β-trypsin	20.7 ± 0.5 (3)[b]	14.5 ± 4.2 (3)[b]	18.2 ± 0.31 (3)	14.1 ± 1.02 (3)	73.4 ± 11 (3)
human plasmin	>1000[b]	>1000	10.6 ± 2.4 (3)	12.5 ± 3.8 (3)	9.8 ± 2.4 (3)
murine plasmin	>1000[b]	>1000	2.97 ± 0.33 (3)	3.42 ± 0.23 (3)	3.67 ± 0.21 (3)
human FXIa	>1000[b]	2.56 ± 0.35 (3)	3.97 ± 0.52 (3)	12.1 ± 1.0 (3)	6.63 ± 0.50 (3)
human KLK1	>1000	>1000	0.201 ± 0.057 (3)	0.384 ± 0.026 (3)	0.833 ± 0.158 (3)

[a]Besides the proteases reported in the table, none of the peptides showed any measurable inhibition (K_i > 1000 μM) in human activated protein C (aPC), human matriptase, human and murine thrombin, or human and murine tissue-type plasminogen activator (tPA). [b]Data from our previously reported work,[20,22] shown here to facilitate comparison.

DOI: 10.1021/acs.jmedchem.5b01128
J. Med. Chem. XXXX, XXX, XXX−XXX

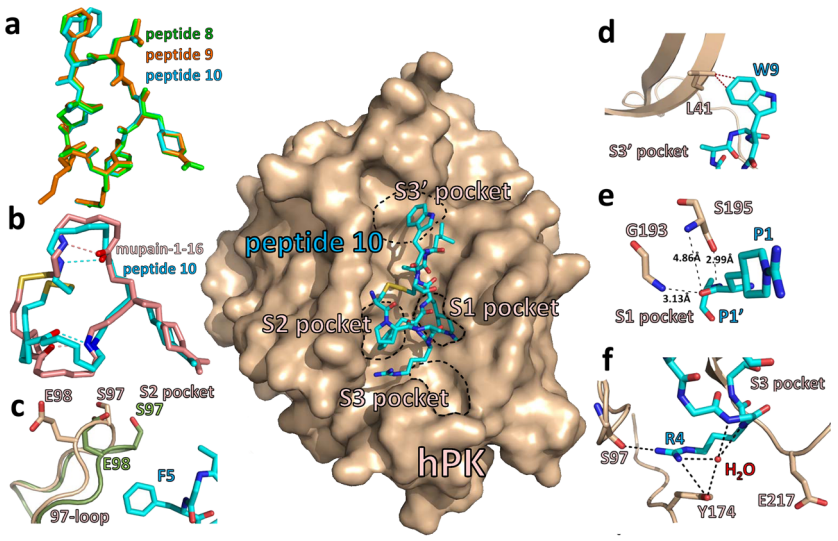

Figure 3. X-ray crystal structure analysis of the peptide **10**:hPK complex (PDB code 4ZJ6). Center: An overview of the structure of peptide **10** (cyan sticks) in complex with catalytic domain of hPK (wheat surface). The S1 pocket and the S2, S3, and S3′ pockets are indicated. Detailed structural information is demonstrated in (a–f). Hydrogen bonds and polar interactions are shown as black dashed lines, and nonpolar interactions are shown as red dashed lines. An H_2O molecule involved in the interactions is shown as red sphere. (a) Peptides **8** (green), **9** (orange), and **10** (cyan) form identical conformations when binding to hPK. (b) The backbone conformations of mupain-1-16 bound to uPA and of peptide **10** bound to PK differ slightly. The tight β-turns are shown as dashed lines. The side chain of P1 residues and the backbones of the two peptides are shown as sticks. The disulfide bonds are colored yellow. (c) S2 pocket: Phe5 docks into the empty S2 pocket and forces the 97-loop to expose to the solvent; the 97-loop of the unbound hPK (smudge, PDB code 2ANY) is aligned for comparison. (d) S3′ pocket: Trp9 of peptide **10** forms hydrophobic interaction with Leu41 of hPK. (e) S1 pocket: the hydroxyl of Ser195 holds a distance of 2.99 Å to the carbonyl carbon of the P1 residue of peptide **10**; the carbonyl oxygen of P1 residue does not dock into the oxyanion hole because of the 4.86 Å distance to the amidogen of Ser195. (f) S3 pocket: Arg4 is stabilized by the polar interaction-network composed by Tyr174, Ser97 and a water molecule instead of binding to Glu217.

Conclusively, beginning with mupain-1, we substituted five residues and improved the affinity to hPK from a K_i value of more than 1000 μM to around 0.01 μM. Simultaneously, the affinity to muPA and huPA-H99Y was completely lost (Figure 1). So we acquired three potent peptide PK inhibitors, peptides **8**, **9**, and **10**, for which we propose the names pkalin-1, pkalin-2, and pkalin-3, respectively. In addition, all of the three PK inhibitors showed remarkable inhibition of mPK, which paves a path for evaluating the activities of the peptides in animal models (Table 1).

Specificity and Biochemical Properties. To study the specificity of the three selected peptides, we measured the K_i values for inhibition of several other serine proteases (Table 1). None of the three PK inhibitors showed measurable inhibition of activated protein C, matriptase, thrombin, tissue-type plasminogen activator. The non-natural P1 residue L-3-(*N*-amidino-4-piperidyl)alanine endows mupain-1-16 with a measurable K_i for human factor XIa (K_i = 2.56 μM), and this affinity was inherited by the PK inhibitors. Also, the affinity of the peptides to plasmin increased significantly after re-engineering of the exosite interactions. The three PK inhibitors also showed measurable inhibition of KLKL-1 with the K_i values in the submicromolar range, possibly related to the fact that KLK1 and PK share a cleavage site in the kininogens.[24] However, compared to the high affinity (K_i values in low nanomolar range) to hPK, the affinity to FXIa, plasmin, and KLK1 is negligible. The results indicate that our retargeting strategy did not give rise to significant off-target inhibition and kept the specificity. Furthermore, the PK inhibitors not only inhibit hydrolysis of the chromogenic substrate but also efficiently inhibit the interaction of hPK and its protein substrates, high molecular weight kininogen (HMWK), and the zymogen of uPA (pro-uPA) (Figure S2).

We considered the possibility that these three peptides were poor inhibitors of these other proteases because the proteases could proteolytically cleave the PK inhibitors instead of being inhibited by them. Using plasmin as an example, we found that plasmin cleaved peptide **10** very slowly, only 0.059%/h·nM plasmin, so slow that it would not account for more than 0.12% cleavage with the plasmin concentrations (2 nM) and incubation times (1 h) used during inhibition assays. Thus, cleavage cannot account for the poor inhibition. We also incubated peptide **8** and peptide **10** in human plasma for various periods of time. After the incubation, we estimated the remaining inhibitory activity. The peptides **8** and **10** were found to be quite stable in plasma, having half-lives of >24 h (Figure S4).

Several artificial inhibitors of hPK have been developed by others before, including *trans*-4-aminomethylcyclohexane-carbonylphenylalanyl-4-carboxymethylanilide (PKSI-527, a small molecular inhibitor),[25] ecallantide (an engineered Kunitz type inhibitor),[26] DX-2930 (a monoclonal antibody),[27] and bicyclic peptidic inhibitors developed in C. Heinis's laboratory.[28−30] Our peptide inhibitors have shown affinity and specificity comparable to monoclonal antibodies, and the small-size monocyclic peptides with only 10 residues have the advantage that they are easy to prepare in large scale.

Studies of the Binding and Inhibitory Mechanism of PK Inhibitors by X-ray Crystal Structure Analysis and Site-Directed Mutagenesis. In order to verify our retargeting strategy, we crystallized the catalytic domain (serine protease domain, SPD) of hPK in complex with each of the three PK inhibitors (Figure 3). The three peptides form identical

DOI: 10.1021/acs.jmedchem.5b01128
J. Med. Chem. XXXX, XXX, XXX−XXX

conformations when binding to hPK-SPD (Figure 3a). Here, the structure of peptide **10** in complex with hPK-SPD (PDB code 4ZJ6) was selected as a representative to illustrate the peptide−hPK interactions.

Sequencewise, peptide **10** (CPARF[L-3-(*N*-amidino-4-piperidyl)alanine]ALWC) has no resemblance to the recognition sites of physiological substrates (HMWK, factor XII, or uPA) or artificial substrates of hPK.[24] Interestingly, peptide **10** binds to hPK in a substrate-like conformation (Figure 3 central) but is not cleaved like a substrate. In the crystal structure, the hydroxyl group of Ser195 holds a distance of 2.99 Å to the carbonyl carbon of the P1 residue (Figure 3e), which is too long for nucleophilic attack. Besides, the carbonyl oxygen of the P1 residue does not dock into the oxyanion hole correctly but is 4.86 Å away from the amino group of Ser195 (Figure 3e). Thus, the tetrahedral intermediate cannot be stabilized by the oxyanion hole in the transition state. These two observations could explain that peptide **10** is an inhibitor but not a substrate. An alternative explanation would be that an acyl-enzyme intermediate can in fact be formed but that the P1′ residue is locked in its original position and thus does not allow access of the water molecule needed for the second step of hydrolysis. Therefore, the original peptide bond will re-form. Such an explanation has been given for the stability of the complex between trypsin and bovine pancreas trypsin inhibitor.[31,32] At the moment, we are unable to distinguish between these two possibilities.

The *N*-amidino-4-piperidyl side chain of the P1 residue inserts into the active site (S1 pocket), and the other parts of peptides stretch out on the enzyme surface and form exosite interactions. The bulky phenylic side chain of Phe5 (the P2 residue) docks into the relatively large S2 pocket and forces the 97-loop outward in contrast to the ligand-free PK (Figure 3c). The hydrophilic side chains of Ser97 and Glu98 are also forced to become exposed to the solvent. That fits the result of site-directed mutagenesis that substituting Gly99 of hPK with Tyr (the corresponding residue of muPA) decreases hPK's affinity to peptide **10** (with a Phe5) 5.6-fold but increases the affinity to mupain-1-16 (with a Ser5) 6.7-fold (Table 2). These results confirm the theory that the size of the 97-loop is critical for the preference for specific P2 residues. In the S3′ pocket, the aromatic Trp9 forms hydrophobic interactions with the isobutyl side chain of Leu41 (Figure 3d). Unlike mupain-1-16, which stretches out flexibly on the surface of huPA-H99Y, the backbone of peptide **10** in hPK is in a more twisted conformation, especially the part around the disulfide bond (Figure 3b). The rigid and bulky Tyr7 in mupain-1-16 hinders this peptide from forming this unfavorable state. In contrast, the much smaller Ala7 of peptide **10** facilitates the folding of the peptide into the twisted conformation. Thus, rather than Tyr, the small-size Ala is the more favorable P1′ residue for PK inhibitors.

Table 2. Effects of Site-Directed Mutagenesis of hPK-SPD on the K_i Values (nM) for Inhibition by Mupain-1-16 and Peptide 10

hPK mutant	mupain-1-16	peptide 10
wild type	907 ± 138 (3)	9.93 ± 1.78 (3)
E217A	938 ± 252 (3)	31.9 ± 5.6 (3)
E217R	1694 ± 78 (3)	166 ± 18 (3)
G99Y	136 ± 14 (3)	53.6 ± 4.6 (3)

The above results of crystallography and site-directed mutagenesis are consistent with the K_i measurements and therefore verify our retargeting strategy. The only fact that does not fit our design strategy is in the S3 pocket. By inserting an Arg as the P3 residue of the peptide, we expected to establish an electrostatic interaction to Glu217 of hPK. But when we inactivated Glu217 by substituting with Ala, only a minor change in the affinity to peptide **10** was observed (Table 2), which indicates that Glu217 of hPK has negligible effect on binding to peptide **10**. However, this result is in agreement with the crystal structure analysis, which shows that the guanidine group of the Arg4 does not bind to Glu217 but stretches to the 97-loop and is stabilized by a sturdy polar interaction network (Figure 3f). Substituting Tyr4 by Arg did drastically decrease the affinity of peptides to the uPAs (Figure 1). Thus, although Arg4 of peptides does not bind to Glu217 of hPK, Arg4 electronically repulsed Arg217 of the uPAs, which is also comfirmed by the 16.8-fold decrease of the affinity of hPK to peptide **10** when substituting Glu217 with Arg (Table 2).

Kinetic Studies of Peptide−Protease Interactions through Surface Plasmon Resonance (SPR) Analysis. The K_D values of peptide **10** and mupain-1-16 binding to hPK are 3.0 and 737 nM, respectively (Table 3). The K_D values are slightly lower than the K_i values from enzymological assays (13.7 nM and 1.58 μM), most likely due to the fact that the SPR analysis was carried out at 25 °C, while the K_i values were determined at 37 °C. Because of the nonmeasurably low affinity (K_i > 1000 μM), the K_D value for mupain-1 binding to hPK could not be determined by SPR. The Gibbs free energy changes (ΔG) for the binding of the peptides to hPK were calculated according to the K_D values. Substitution of the P1 residue (Arg 6) with L-3-(*N*-amidino-4-piperidyl)alanine in the active site contributes a binding energy change of $\Delta(\Delta G)$ > 17.9 kJ/mol (from mupain-1 to mupain-1-16), while re-engineering the exosite interactions by replacing four residues contributes only a binding energy change of $\Delta(\Delta G)$ = 13.6 kJ/mol (from mupain-1-16 to peptide **10**). Therefore, the change in the active site interaction plays an energetically more important role in engineering the affinity of peptide to hPK. But this change in the active site indiscriminately improves the

Table 3. Analysis of Peptide−Protease Binding by SPR Analysis[a]

protease	peptide	$k_{on} \times 10^{-5}$ (M^{-1} s^{-1})	$k_{off} \times 10^{2}$ (s^{-1})	K_D (nM)	ΔG (kJ/mol)
hPK	mupain-1	no measurable binding		> 10^6	>−17.1
hPK	mupain-1-16	kinetics could not be fitted		737 ± 86 (3)	−35.0
hPK	peptide **10**	102 ± 23 (3)	2.88 ± 0.22 (3)	3.04 ± 0.86 (3)	−48.6

[a]The K_D values were calculated by both kinetic and steady-state methods. Due to the very low affinity to PK, mupain-1 could not be studied by SPR. The association and dissociation rates for mupain-1-16 binding to hPK could not be fitted, but the K_D value was instead calculated by the steady state affinity measurement. The binding of peptide **10** to hPK agreed with a 1:1 binding model. The ΔG values were calculated according to the equation $\Delta G = RT \ln K_D$.

DOI: 10.1021/acs.jmedchem.5b01128
J. Med. Chem. XXXX, XXX, XXX−XXX

peptides' inhibitory capability of many serine proteases, not only PKs but also factor XIa, the uPAs, and the plasmins (Table 1). Thus, the active site (P1−S1) interactions are critical for the affinity but have a minor contribution to specificity among different proteases. In contrast, re-engineering of the exosite interactions allows the change in specificity.

Designing Inhibitors of Serine Proteases Based on the Scaffold of Mupain-1. The present conversion of the uPA inhibitor to a PK inhibitor suggests that the mupain-1 scaffold may be useful as a basis for generating high specificity and high affinity inhibitors of also other trypsin-like serine proteases. A scaffolding approach has previously been used to design inhibitors of various serine proteases on the basis of the 12 residues long sunflower trypsin inhibitor.[33−35] From the crystal structures of the mupain-1-16:huPA-H99Y and peptide **10**:hPK complexes, we can summarize the common conformation of the mupain-1-derived peptides in complexes with each of the two enzymes in the following way: Residues 4−9 form intimate contacts with the enzyme and bind as P3, P2, P1, P1′, P2′, and P3′ residues, respectively, while residues 1−3 and residue 10 are solvent exposed and form very few interactions with the enzymes (Figures 4, S5, and S6). The structures also

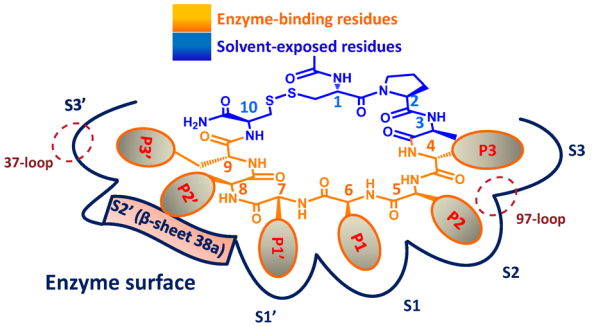

Figure 4. Model for mupain-1 as a versatile scaffold for design of serine protease inhibitors. The small 10-mer cyclic peptide, mupain-1, is suggested as a useful scaffold for targeting different proteases. The interactions of individual mupain-1-derived peptides with the surface of serine proteases are indicated. Protease-binding residues and solvent-exposed residues are shown in blue and orange, respectively.

indicate that mupain-1-16 and peptide **10** have identical backbone conformation in the residues 4−9, while the backbones of residues 1−3 and 10 vary. Retargeting mupain-1 to another serine protease would therefore implicate keeping residues 1−3 and 10 constant while changing residues 4−9 to obtain an optimal binding to the serine protease in question, either by rational or by stochastic engineering. This suggestion rests on the assumption that residues 1−3 and 10 provides a scaffold that, when kept constant, will facilitate retargeting, as compared to beginning with a totally randomized X_{10} library; the constant region may help to present the other residues in a manner suitable for binding to trypsin serine proteases. First, the disulfide bridge of Cys1 and Cys10 provides a necessary circular structure, as the corresponding linear peptides are inactive.[19] Second, the position in the sequence of the energetically and functionally important P1 residue relative to the enzyme-binding and the surface-exposed residues are indispensable. Third, Pro2 is crucial because the rigidity of this residue is conformationally important for peptides and proteins.[36] Fourth, the two tight β-turns in both muPA and PK inhibitors also constrain the peptides to the necessary conformation. Fifth, the main chain of the peptide is sufficiently flexible to absorb small changes following substitution of the enzyme binding residues while still allowing an overall inhibitory binding mode, as shown by the slightly different main chain conformations of mupain-1 in complex with huPA H99Y and peptide **10** in complex with hPK (Figure 3b).

Here, we used rational design for retargeting. In most cases, it may be more favorable to use a stochastic approach, randomizing several or all of the enzyme-binding residues. In fact, we recently designed a new library screening strategy consisting of a back-flip library of peptide−protease fusions and thereby generated a mupain-1 derivative with an increased affinity to muPA (2 nM) and a moderate affinity to huPA wild type (530 nM).[37] Directed evolution also offers the opportunity of counterselections in order to reduce affinity to nontarget proteases. Also, it handles the unpredictability inherent in rational design caused by the fact that the effect exchange of the residue in one position may not be independent of exchanges of residues in other positions and that the enzyme may be flexible.[20,37]

CONCLUSIONS

To achieve highly specific serine protease inhibitors, we report here a strategy based on a versatile short peptide scaffold, mupain-1. We retargeted this original muPA inhibitor to another trypsin-like serine protease, plasma kallikrein. By simply substituting five residues of the 10-mer peptide, we engineered high-affinity hPK inhibitors with K_i values around 0.01 μM. The hPK inhibitors also showed remarkable specificity. By studying the binding and inhibitory mechanism of the PK inhibitors, we verified the authenticity of the designing strategy. We suggest that mupain-1 may be used as a scaffold for designing high-affinity, high-specificity inhibitors of other serine proteases.

EXPERIMENTAL SECTION

General. General chemicals were purchased from Sigma-Aldrich (St. Louis, MO, USA), Iris Biotech GmbH (Marktredwitz, Germany), or Rapp Polymere GmbH (Tübingen, Germany) and used without further purification unless otherwise stated. Full-length human and murine plasma kallikrein, plasmin, and thrombin were purchased from Molecular Innovation (Novi, MI, USA). Bovine β-trypsin was purchased from Roche Applied Science (Penzburg, Germany). Human activated protein C was purchased from Maxygen (CA, USA). KLK1 was purchased from ProSpec-Tany Technogene Ltd. (New Jersey, USA). The peptides were synthesized by Wuxi PharmaTech (Shanghai, China). Fmoc-L-3-(*N*-amidino-4-piperidyl)-alanine was prepared as described in our previous work.[22] The quality of peptides was estimated with HPLC and mass spectra (Figure S7). The purity of all peptides are >95% according to the analytical HPLC results.

Determination of K_i Values. For routine determination of K_i values for the inhibition of the various enzymes under steady state inhibition conditions, 2 nM purified enzyme was preincubated in a total volume of 200 μL of 0.01 M Hepes, 0.14 M NaCl, pH 7.4 with 0.1% BSA at 37 °C, with various concentrations of peptides for 15 min prior to the addition of the chromogenic substrate (S-2444 (pyro-Glu-Gly-Arg-*p*-nitroanilide) for the uPA variants; S-2302 (H-D-Pro-Phe-Arg-*p*-nitroanilide) for the PK variants; S-2288 (H-D-Ile-Pro-Arg-*p*-nitroanilide) for human activated protein C, human matriptase, human tPA, human and murine plasmin, and human and murine thrombin; S-2765 (Z-D-Arg-Gly-Arg-*p*-nitroanilide) for murine tPA; S-2222 (Bz-Ile-Glu(g-OR)-Gly-Arg-*p*-nitroanilide) for bovine β-trypsin; S-2251 (Val-Leu-Lys-*p*-nitroanilide) for KLK1) in concentrations approximately equal to the K_M value for each particular variant. The initial reaction velocities were monitored at an absorbance of 405 nm. The inhibition constants (K_i) were subsequently determined from the

DOI: 10.1021/acs.jmedchem.5b01128
J. Med. Chem. XXXX, XXX, XXX−XXX

nonlinear regression analyses of plots of V_i/V_0 versus $[I]_0$, using eq 1, derived under assumption of competitive inhibition:

$$\frac{V_i}{V_0} = \frac{K_i([K_M + [S]_0)}{K_i[S]_0 + K_M(K_i + [I]_0)} \quad (1)$$

V_i and V_0 are the reaction velocities in the presence and absence of inhibitor, respectively; $[S]_0$ and $[I]_0$ are the substrate and inhibitor concentrations, respectively; K_M is K_M for substrate hydrolysis by each protease. In eq 1, it is assumed that $[S] \approx [S]_0$ and $[I] \approx [I]_0$. These conditions were fulfilled, as less than 10% of the substrate was converted to product in the assays and as the assay typically contained a final concentration of each protease of 2 nM and inhibitor concentrations of >5 nM.

Production of Recombinant Proteins. Wild-type and mutated recombinant human and murine uPA were expressed in HEK (human embryonic kidney)-293T cells with the vector pcDNA3.1 (−) harboring full-length uPA genes.[20] The catalytic domain of human matriptase and fXIa was expressed in *Pichia pastoris* strain X-33 as described before.[38]

The plasmid of wild-type catalytic domain of human plasma kallikrein (hPK-SPD) was constructed as described in the work of Tang et al.[39] cDNA sequence encoding the hPK-SPD, from Asn357 to Ala619 (based on the numbering system of mature prekallikrein, signal sequence not included), in which Cys364 and Cys484 were mutagenized to serines, was inserted into PICZαA vector. Mutations were induced by using the QuikChange site-directed mutagenesis kit. The plasmids containing wild-type or mutated hPK-SPD were transfected into *Pichia pastoris* yeast strain, X-33. Expression of the variants was induced by methanol. The protein was purified with a cation exchange column (SP Sepharose Fast Flow, SPFF, GE Healthcare, Uppsala, Sweden), followed by gel filtration chromatography (Superdex 75 HR 10/30, Pharmacia Biotech). The purity of the recombinant hPK-SPD proteins was certified with SDS−PAGE (Figure S1).

Crystallization and Structure Determination. Peptides **8**, **9**, and **10** in complexes with hPK-SPD were crystallized from sitting drops, composed of 0.5 μL of the mix and 0.5 μL of the reservoir solution. The reservoir solutions for crystallizing hPK-SPD in complexes with the three peptides were 28% PEG3350, 0.1 M Tris-HCl, pH 8.5, 20 mM $(NH_4)_2SO_4$; 25% PEG3350, 0.1 M HEPES, pH 7.5, 20 mM $(NH_4)_2SO_4$; 23% PEG3350, 0.1 M Tris-HCl, pH8.5, 20 mM $(NH_4)_2SO_4$, respectively; crystals grew within 5 days at 25 °C. The reservoir solutions with 25% (v/v) glycerol were used as cryoprotectants used before data collection.

X-ray diffraction data were collected at 100 K on SER-CAT 22-ID beamline at Advanced Photon Source (Argonne National Laboratory, Argonne, IL, USA) and BL17U beamline at Shanghai Synchrotron Radiation Facility (SSRF, China). The crystal structures were solved by molecular replacement using Molrep software of the CCP4 program suite[40] and the published catalytic domain of hPK (PDB code 2ANY) as the search model. The $F_O - F_C$ electron density map revealed clear extra electron density for peptides at the active site of hPK-SPD in the complexes and was modeled by the known peptide sequences. The models were then manually adjusted by COOT[41] and refined by REFMAC.[40] After the final cycles of refinement using REFMAC of CCP4, the models have reasonable statistics (Table S4) and geometries with only one residue in the disallowed region of the Ramachandran plots. The structures of hPK-SPD in complexes with peptides **8**, **9**, and **10** have been deposited to the RCSB PDB database (4ZJ4, 4ZJ5, and 4ZJ6).

Surface Plasmon Resonance (SPR) Analysis. To determine the equilibrium binding constants (K_D), the association rate constants (k_{on}), and dissociation rate constants (k_{off}) for peptide binding to full-length plasma kallikrein, surface plasmon resonance analysis was performed on a BIACORE T200 instrument (BIACORE, Uppsala, Sweden). A CM5 chip was coupled with hPK by injecting the enzyme in a concentration of 30 μg/mL in immobilization buffer (10 mM sodium acetate, pH 5.0), aiming for an immobilized level of approximately 500 response units (RU). Immobilization was followed by surface blocking with ethanolamine. A reference cell was prepared in the same way, without coupling of hPK. Running buffer containing peptidic inhibitors in a dilution series was injected at a flow rate of 30 μL per min during 90 s at 25 °C. Subsequently, the dissociation was monitored during 300 s. Kinetic constants (k_{on} and k_{off}) were calculated with the BIACORE evaluation software, using the 1:1 kinetic fit. The K_D values were calculated as k_{off}/k_{on}.

■ ASSOCIATED CONTENT

Supporting Information

The Supporting Information is available free of charge on the ACS Publications website at DOI: 10.1021/acs.jmedchem.5b01128.

Additional experimental information, sequences, and the K_i values of all peptides involved in this work, production of recombinant proteins, figures with sensorgrams from SPR analysis, the effects of the PK inhibitors on the activity of PK toward protein substrates, stability of peptides **8** and **10** in human plasma crystallographic parameters, and other results referred in the text (PDF)

Accession Codes

The PDB codes for the structures of peptides **8** (pkalin-1), **9** (pkalin-2), and **10** (pkain-3) in complexes with hPK-SPD are 4ZJ4, 4ZJ5, and 4ZJ6, respectively.

■ AUTHOR INFORMATION

Corresponding Author

*Phone: +45 8715 5456. E-mail: pa@mb.au.dk.

Notes

The authors declare no competing financial interest.

■ ACKNOWLEDGMENTS

This work was supported by the Danish National Research Foundation (Grant 26-331-6 to P.A.A.), the Natural Science Foundation of China (Grants 31161130356, 31170707, 31370737 to M.H.), the Natural Science Foundation of the Fujian Province (Grant 2012J05071 to L.J.), the Lundbeck Foundation (Grant R83-A7826 to P.A.A.), the Carlsberg Foundation (Grant 2012_01_0642 to P.A.A.), and the Cancer Research Foundation of 1989 (to P.A.A.). P.A.A. was awarded a Chinese Academy of Sciences visiting professorship for senior international scientists (Grant 2012T1G0023). M.H. was awarded an Aarhus University Research Foundation visiting professorship (Reference Number 10). The funders had no role in study design, data collection and analysis, decision to publish, or preparation of the manuscript.

■ ABBREVIATIONS USED

PK, plasma kallikrein; hPK, human plasma kallikrein; mPK, murine plasma kallikrein; uPA, urokinase-type plasminogen activator; huPA, human urokinase-type plasminogen activator; muPA, murine urokinase-type plasminogen activator; HMWK, high molecular weight kininogen; HAE, hereditary angioedema; K_i, inhibitory constant; K_D, dissociation constant; SPD, serine protease domain; RU, response unit; SPR, surface plasmon resonance; BSA, bovine serum albumin

■ REFERENCES

(1) Puente, X. S.; Ordóñez, G. R.; López-Otín, C. Protease Genomics and the Cancer Degradome. In *The Cancer Degradome*, 1st ed.; Edwards, D., Høyer-Hansen, G., Blasi, F., Sloane, B. F., Eds.; Springer New York: New York, 2008; pp 3−15.

DOI: 10.1021/acs.jmedchem.5b01128
J. Med. Chem. XXXX, XXX, XXX−XXX

(2) Turk, B. Targeting Proteases: Successes, Failures and Future Prospects. *Nat. Rev. Drug Discovery* **2006**, *5*, 785−799.
(3) Cudic, M.; Fields, G. B. Extracellular Proteases as Targets for Drug Development. *Curr. Protein Pept. Sci.* **2009**, *10*, 297−307.
(4) Drag, M.; Salvesen, G. S. Emerging Principles in Protease-Based Drug Discovery. *Nat. Rev. Drug Discovery* **2010**, *9*, 690−701.
(5) Coussens, L. M.; Fingleton, B.; Matrisian, L. M. Matrix Metalloproteinase Inhibitors and Cancer: Trials and Tribulations. *Science* **2002**, *295*, 2387−2392.
(6) Birkedalhansen, H.; Moore, W. G. I.; Bodden, M. K.; Windsor, L. J.; Birkedalhansen, B.; Decarlo, A.; Engler, J. A. Matrix Metalloproteinases: A Review. *Crit. Rev. Oral Biol. Med.* **1993**, *4*, 197−250.
(7) Krowarsch, D.; Cierpicki, T.; Jelen, F.; Otlewski, J. Canonical Protein Inhibitors of Serine Proteases. *Cell. Mol. Life Sci.* **2003**, *60*, 2427−2444.
(8) Huntington, J. A. Shape-Shifting Serpins - Advantages of a Mobile Mechanism. *Trends Biochem. Sci.* **2006**, *31*, 427−435.
(9) Overall, C. M. Molecular Determinants of Metalloproteinase Substrate Specificity - Matrix Metalloproteinase Substrate Binding Domains, Modules, and Exosites. *Mol. Biotechnol.* **2002**, *22*, 51−86.
(10) Page, M. J.; MacGillivray, R. T. A.; Di Cera, E. Determinants of Specificity in Coagulation Proteases. *J. Thromb. Haemostasis* **2005**, *3*, 2401−2408.
(11) Craik, D. J.; Fairlie, D. P.; Liras, S.; Price, D. The Future of Peptide-Based Drugs. *Chem. Biol. Drug Des.* **2013**, *81*, 136−147.
(12) Dennis, M. S.; Eigenbrot, C.; Skelton, N. J.; Ultsch, M. H.; Santell, L.; Dwyer, M. A.; O'Connell, M. P.; Lazarus, R. A. Peptide Exosite Inhibitors of Factor VIIa as Anticoagulants. *Nature* **2000**, *404*, 465−470.
(13) Dennis, M. S.; Roberge, M.; Santell, L.; Dwyer, M. A.; Eigenbrot, C.; Skelton, N. J.; Lazarus, R. A. Two Distinct Classes of Peptide Exosite Inhibitors of Factor VIIa as Anticoagulants. *Blood* **2000**, *96*, 261a−261a.
(14) Lin, J.; Deng, H. F.; Jin, L.; Pandey, P.; Quinn, J.; Cantin, S.; Rynkiewicz, M. J.; Gorga, J. C.; Bibbins, F.; Celatka, C. A.; Nagafuji, P.; Bannister, T. D.; Meyers, H. V.; Babine, R. E.; Hayward, N. J.; Weaver, D.; Benjamin, H.; Stassen, F.; Abdel-Meguid, S. S.; Strickler, J. E. Design, Synthesis, and Biological Evaluation of Peptidomimetic Inhibitors of Factor XIa as Novel Anticoagulants. *J. Med. Chem.* **2006**, *49*, 7781−7791.
(15) Baeriswyl, V.; Calzavarini, S.; Gerschheimer, C.; Diderich, P.; Angelillo-Scherrer, A.; Heinis, C. Development of a Selective Peptide Macrocycle Inhibitor of Coagulation Factor XII toward the Generation of a Safe Antithrombotic Therapy. *J. Med. Chem.* **2013**, *56*, 3742−3746.
(16) Bock, P. E.; Day, D. E.; Verhamme, I. M. A.; Bernardo, M. M.; Olson, S. T.; Shore, J. D. Analogs of Human Plasminogen that are Labeled with Fluorescence Probes at the Catalytic Site of the Zymogen - Preparation, Characterization, and Interaction with Streptokinase. *J. Biol. Chem.* **1996**, *271*, 1072−1080.
(17) Botkjaer, K. A.; Byszuk, A. A.; Andersen, L. M.; Christensen, A.; Andreasen, P. A.; Blouse, G. E. Nonproteolytic Induction of Catalytic Activity into the Single-Chain Form of Urokinase-Type Plasminogen Activator by Dipeptides. *Biochemistry* **2009**, *48*, 9606−9617.
(18) Landgraf, K. E.; Santell, L.; Billeci, K. L.; Quan, C.; Young, J. C.; Maun, H. R.; Kirchhofer, D.; Lazarus, R. A. Allosteric Peptide Activators of Pro-Hepatocyte Growth Factor Stimulate Met Signaling. *J. Biol. Chem.* **2010**, *285*, 40362−40372.
(19) Andersen, L. M.; Wind, T.; Hansen, H. D.; Andreasen, P. A. A Cyclic Peptidylic Inhibitor of Murine Urokinase-Type Plasminogen Activator: Changing Species Specificity by Substitution of a Single Residue. *Biochem. J.* **2008**, *412*, 447−457.
(20) Zhao, B.; Xu, P.; Jiang, L.; Paaske, B.; Kromann-Hansen, T.; Jensen, J. K.; Sorensen, H. P.; Liu, Z.; Nielsen, J. T.; Christensen, A.; Hosseini, M.; Sorensen, K. K.; Nielsen, N. C.; Jensen, K. J.; Huang, M.; Andreasen, P. A. A Cyclic Peptidic Serine Protease Inhibitor: Increasing Affinity by Increasing Peptide Flexibility. *PLoS One* **2014**, *9*, e115872.
(21) Zuraw, B. L. Hereditary Angioedema. *N. Engl. J. Med.* **2008**, *359*, 1027−1036.
(22) Hosseini, M.; Jiang, L. G.; Sorensen, H. P.; Jensen, J. K.; Christensen, A.; Fogh, S.; Yuan, C.; Andersen, L. M.; Huang, M. D.; Andreasen, P. A.; Jensen, K. J. Elucidation of the Contribution of Active Site and Exosite Interactions to Affinity and Specificity of Peptidylic Serine Protease Inhibitors Using Non-Natural Arginine Analogs. *Mol. Pharmacol.* **2011**, *80*, 585−597.
(23) Benfield, A. P.; Teresk, M. G.; Plake, H. R.; DeLorbe, J. E.; Millspaugh, L. E.; Martin, S. F. Ligand Preorganization may be Accompanied by Entropic Penalties in Protein-Ligand Interactions. *Angew. Chem., Int. Ed.* **2006**, *45*, 6830−6835.
(24) Pathak, M.; Wong, S. S.; Dreveny, I.; Emsley, J. Structure of Plasma and Tissue Kallikreins. *Thromb. Haemostasis* **2013**, *110*, 423−433.
(25) Okada, Y.; Tsuda, Y.; Tada, M.; Wanaka, K.; Hijikata-Okunomiya, A.; Okamoto, U.; Okamoto, S. Development of Plasma Kallikrein Selective Inhibitors. *Biopolymers* **1999**, *51*, 41−50.
(26) Levy, J. H.; O'Donnell, P. S. The Therapeutic Potential of a Kallikrein Inhibitor for Treating Hereditary Angioedema. *Expert Opin. Invest. Drugs* **2006**, *15*, 1077−1090.
(27) Kenniston, J. A.; Faucette, R. R.; Martik, D.; Comeau, S. R.; Lindberg, A. P.; Kopacz, K. J.; Conley, G. P.; Chen, J.; Viswanathan, M.; Kastrapeli, N.; Cosic, J.; Mason, S.; DiLeo, M.; Abendroth, J.; Kuzmic, P.; Ladner, R. C.; Edwards, T. E.; TenHoor, C.; Adelman, B. A.; Nixon, A. E.; Sexton, D. J. Inhibition of Plasma Kallikrein by a Highly Specific Active Site Blocking Antibody. *J. Biol. Chem.* **2014**, *289*, 23596−23608.
(28) Heinis, C.; Rutherford, T.; Freund, S.; Winter, G. Phage-encoded Combinatorial Chemical Libraries Based on Bicyclic Peptides. *Nat. Chem. Biol.* **2009**, *5*, 502−507.
(29) Baeriswyl, V.; Rapley, H.; Pollaro, L.; Stace, C.; Teufel, D.; Walker, E.; Chen, S.; Winter, G.; Tite, J.; Heinis, C. Bicyclic Peptides with Optimized Ring Size Inhibit Human Plasma Kallikrein and its Orthologues while Sparing Paralogous Proteases. *ChemMedChem* **2012**, *7*, 1173−1176.
(30) Baeriswyl, V.; Heinis, C. Phage Selection of Cyclic Peptide Antagonists with Increased Stability toward Intestinal Proteases. *Protein Eng., Des. Sel.* **2013**, *26*, 81−89.
(31) Zakharova, E.; Horvath, M. P.; Goldenberg, D. P. Structure of a Serine Protease Poised to Resynthesize a Peptide Bond. *Proc. Natl. Acad. Sci. U. S. A.* **2009**, *106*, 11034−11039.
(32) Hamada, Y.; Ishiura, S.; Kiso, Y. BACE1 Inhibitor Peptides: Can an Infinitely Small k(cat) Value Turn the Substrate of an Enzyme into Its Inhibitor? *ACS Med. Chem. Lett.* **2012**, *3*, 193−197.
(33) Zablotna, E.; Jaskiewicz, A.; Legowska, A.; Miecznikowska, H.; Lesner, A.; Rolka, K. Design of Serine Proteinase Inhibitors by Combinatorial Chemistry Using Trypsin Inhibitor SFTI-1 as a Starting Structure. *J. Pept. Sci.* **2007**, *13*, 749−755.
(34) de Veer, S. J.; Ukolova, S. S.; Munro, C. A.; Swedberg, J. E.; Buckle, A. M.; Harris, J. M. Mechanism-Based Selection of a Potent Kallikrein-Related Peptidase 7 Inhibitor From a Versatile Library Based on the Sunflower Trypsin Inhibitor SFTI-1. *Biopolymers* **2013**, *100*, 510−518.
(35) Fittler, H.; Avrutina, O.; Empting, M.; Kolmar, H. Potent Inhibitors of Human Matriptase-1 Based on the Scaffold of Sunflower Trypsin Inhibitor. *J. Pept. Sci.* **2014**, *20*, 415−420.
(36) Wedemeyer, W. J.; Welker, E.; Scheraga, H. A. Proline cis-trans Isomerization and Protein Folding. *Biochemistry* **2002**, *41*, 14637−14644.
(37) Sorensen, H. P.; Xu, P.; Jiang, L.; Kromann-Hansen, T.; Jensen, K. J.; Huang, M.; Andreasen, P. A. Selection of High-Affinity Peptidic Serine Protease Inhibitors with Increased Binding Entropy from a Back-Flip Library of Peptide-Protease Fusions. *J. Mol. Biol.* **2015**, *427*, 3110−3122.
(38) Jiang, L. G.; Yuan, C.; Chen, H. W.; Wang, Y.; Zhao, B. Y.; Zhang, X.; Huang, M. D. Preparation and Structure of a New Coagulation Factor XI Catalytic Domain for Drug Discovery. *Chin. J. Struct. Chem.* **2011**, *30*, 1021−1029.

DOI: 10.1021/acs.jmedchem.5b01128
J. Med. Chem. XXXX, XXX, XXX−XXX

(39) Tang, J.; Yu, C. L.; Williams, S. R.; Springman, E.; Jeffery, D.; Sprengeler, P. A.; Estevez, A.; Sampang, J.; Shrader, W.; Spencer, J.; Young, W.; McGrath, M.; Katz, B. A. Expression, Crystallization, and Three-Dimensional Structure of the Catalytic Domain of Human Plasma Kallikrein. *J. Biol. Chem.* **2005**, *280*, 41077−41089.
(40) The CCP4 Suite: Programs for Protein Crystallography. *Acta Crystallogr., Sect. D: Biol. Crystallogr.* **1994**, *50*, 760−763.10.1107/S0907444994003112
(41) Emsley, P.; Cowtan, K. Coot: Model-Building Tools for Molecular Graphics. *Acta Crystallogr., Sect. D: Biol. Crystallogr.* **2004**, *60*, 2126−2132.

DOI: 10.1021/acs.jmedchem.5b01128
J. Med. Chem. XXXX, XXX, XXX−XXX